CHALMERS

FINITE ELEMENT CENTER

PREPRINT 2005–08

Continuum gradient based shape optimization of conducting shields for power frequency magnetic field mitigation

Yueqiang Liu, P. Sousa Jr., E. Salinas, P. Cruz, J. Daalder

Chalmers Finite Element Center
CHALMERS UNIVERSITY OF TECHNOLOGY
Göteborg Sweden 2005

CHALMERS FINITE ELEMENT CENTER

Preprint 2005–08

Continuum gradient based shape optimization of conducting shields for power frequency magnetic field mitigation

Yueqiang Liu, P. Sousa Jr., E. Salinas, P. Cruz, J. Daalder

CHALMERS

Chalmers Finite Element Center
Chalmers University of Technology
SE–412 96 Göteborg Sweden
Göteborg, December 2005

Continuum gradient based shape optimization of conducting shields for power frequency magnetic field mitigation
Yueqiang Liu, P. Sousa Jr., E. Salinas, P. Cruz, J. Daalder
NO 2005–08
ISSN 1404–4382

Chalmers Finite Element Center
Chalmers University of Technology
SE–412 96 Göteborg
Sweden
Telephone: +46 (0)31 772 1000
Fax: +46 (0)31 772 3595
www.phi.chalmers.se

Printed in Sweden
Chalmers University of Technology
Göteborg, Sweden 2005

CONTINUUM GRADIENT BASED SHAPE OPTIMIZATION OF CONDUCTING SHIELDS FOR POWER FREQUENCY MAGNETIC FIELD MITIGATION

YUEQIANG LIU, P. SOUSA JR., E. SALINAS, P. CRUZ, J. DAALDER

Abstract. A shape optimization technique for quasi-static field problems has been developed. The optimization is based on computing the continuum sensitivity function by solving an adjoint problem. We show how this technique can be used to compute, in a very efficient way, the optimal shape of a conducting (or ferromagnetic) shielding structure, in order to minimize the magnetic field in the region of interest. A 2D example of shielding three-phase underground cables is considered.

1. Introduction

Possible adverse health effects due to power frequency magnetic fields have been an issue of great concern in the past two decades. Significant amount of research has been carried out on how to reduce or mitigate the fields [1][2][3][4]. One way is to shield the fields from the sources by using conducting or ferromagnetic plates. An economical solution is to optimize the shape of the plates to achieve the maximal field reduction with a minimal amount of shielding material. The continuum gradient based optimization offers the most efficient way for shape optimization, since the gradient with respect to all the design parameters is computed with maximum two function evaluations (one for the direct problem, and the other for the adjoint problem). Minimizing the number of function evaluations is crucial for solving large (3D) eddy current problems. So far, the continuum gradient has mostly been used for magnetostatic problems [5][6] [7]. This paper focuses on shape optimization for quasi-static low frequency problems using continuum sensitivity computed from the adjoint problems.

Date: December 16, 2005.

Key words and phrases. Optimization methods, Continuum gradient, Magnetic shielding, Eddy currents.

Yueqiang Liu, Department of Applied Mechanics, Chalmers University of Technology, S–412 96 Göteborg, Sweden, *email*: yueqiang.liu@chalmers.se

P. Sousa Jr. is with the Department of Electrical Engineering, Itajuba Federal University, Itajuba, Brazil (*email*: paulo0683@yahoo.com.br)

E. Salinas is with the Faculty of Engineering, Science and the Building Environment, London South Bank University, London, UK (*email*: salinae@lsbu.ac.uk)

P. Cruz is with the Faculty of Electrical Engineering, University of Seville, Spain (*email*: plcruz@us.es)

J. Daalder is with the Department of Electric Power Engineering, Chalmers University of Technology, S-41296, Göteborg, Sweden (*email*: jaap.daalder@chalmers.se).

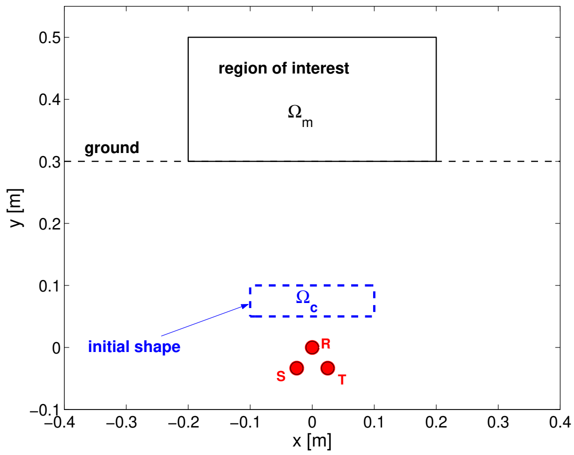

FIGURE 1. Geometry of the magnetic field shielding using a conductor. A rectangular initial shape of the conductor is assumed.

2. PROBLEM DESCRIPTION

An example of the field mitigation is shown in Fig. 1, where a shielding plate (Ω_c) is placed above a system of three-phase underground cables. The general goal is to reduce the magnetic field in the region of interest (Ω_m). The corresponding eddy current problem is formulated for the z-component of the magnetic vector potential $A_z(x,y)$

$$-\nabla \cdot \frac{1}{\mu}\nabla A_z + j\omega\sigma A_z = J_z, \tag{2.1}$$

where $\mu = \mu_c$ and $\sigma = \sigma_c$ in the shielding plate, $\mu = \mu_0$ and $\sigma = 0$ in other regions (for simplicity the underground is simulated as free-space), $\omega = 2\pi f$ with $f = 50$Hz. For an aluminum shielding plate, we use $\sigma_c = 3.774e+7$S/m and $\mu_c = \mu_0$. We assume a uniform distribution of the source current density J_z in the three-phase cables, with $J_z^R = J_0, J_z^S = J_0 e^{j120^o}, J_z^T = J_0 e^{j240^o}$. A total current of 100A flows in each cable of diameter 0.02m. [The skin depth of aluminum is about 1.16cm at 50Hz.]

We define the objective function as

$$\mathcal{E} = w_m \frac{1}{2\mu_0}\int_{\Omega_m} |\nabla \times (A_z\vec{z})|^2 d\Omega + w_c \frac{\omega\sigma}{2}\int_{\Omega_c} |A_z|^2 d\Omega, \tag{2.2}$$

where the first term corresponds to the magnetic energy, with a weighting factor w_m, in the region of interest Ω_m. The second term in Eq. (2.2) is the dissipated energy in the conductor Ω_c, with a weight w_c.

The general shape of the conductor is defined by the shape of the lower boundary and the thickness. The former is parameterized as

$$y_1(x) = \sum_{n=0}^{N} d_n P_n\left(\frac{x}{x_0}\right), \qquad -x_0 \le x \le x_0, \tag{2.3}$$

where the basis functions P_n are chosen as Legendre polynomials. [We also tested Fourier functions, which sometimes result in a worse convergence.] The thickness (measured perpendicularly to lower boundary) of the conductor is parameterized using the same basis functions.

$$h(x) = \sum_{m=0}^{M} g_m P_m\left(\frac{x}{x_0}\right), \qquad -x_0 \le x \le x_0, \tag{2.4}$$

The design parameter vector $\vec{c}$ is defined as $\vec{c} \equiv \{x_0, g_0, g_1, \cdots, g_M, d_0, d_1, \cdots, d_N\}$. Such a parameterization allows us to optimize both the shape and position of the shield.

For optimization, we apply linear constraints on the upper boundary of the conductor: $y_2(x) \le y_{\max} \forall x \in [-x_0, x_0]$, and on the thickness of the conductor: $h(x) \ge h_{\min} \forall x \in [-x_0, x_0]$. We also apply nonlinear constraints on the total area of the conductor: $A_{\text{conduc}} \le A_{\max}$ and on the curvature $\kappa(x)$ of the lower boundary: $\max_x[\kappa(x)h(x)] \le C_{\max}$. The last constraint prevents the optimizer from producing incorrect shapes for the conductor.

We define two reference cases with symmetric and asymmetric shapes, respectively. For the asymmetric case, $N = 6$ in Eq. (2.3). For the symmetric case, only Legendre polynomials with $n = 0, 2, 4, 6$ are included in Eq. (2.3). Other parameters for these two cases are fixed as $w_m = 1, w_c = 0.001, M = 0, y_{\max} = 0.29\text{m}, h_{\min} = 0.005\text{m}, A_{\max} = 0.01\text{m}^2, C_{\max} = 0.95$. We also study non-reference cases by varying parameters $N, M, w_c, A_{\max}$.

3. Computing continuum sensitivity

We give a short derivation of the sensitivity function for the 2D case. Our goal is to compute the first variation, $\delta\mathcal{E}$, of the total energy $\mathcal{E}$, with respect to a small normal displacement $d\xi$ of the boundary of the conducting plate $\Gamma \equiv \partial\Omega_c$.

$$\begin{aligned}\delta\mathcal{E} = {} & w_m \frac{1}{\mu_0} \Re\left\{ \int_{\Omega_m} \left[\nabla \times (A_z^* \vec{z}) \cdot \nabla \times (\delta A_z \vec{z})\right] d\Omega \right\} \\ & + w_c \omega\sigma \Re\left\{ \int_{\Omega_c} A_z^* \cdot \delta A_z d\Omega \right\} + w_c \frac{\omega\sigma}{2} \int_{\Gamma} |A_z|^2 d\xi d\Gamma.\end{aligned} \tag{3.1}$$

In Eq. (3.1), $\Re$ denotes the real part of a complex number, * denotes complex conjugate, δA_z is variation of the solution A_z due to variation of the conductor's shape. Note that the last term in (3.1) is computed straightforward, as soon as we know the solution A_z. We compute the first and the second terms in Eq. (3.1) by solving Eq. (2.1) and an adjoint problem.

The direct problem (2.1) is solved using finite element formulation

$$\mathcal{L}(A_z, \Phi) \equiv \int_{\Omega} \frac{1}{\mu} \nabla A_z \cdot \nabla \Phi + j\omega\sigma A_z \cdot \Phi d\Omega = \int_{\Omega_s} J_z \cdot \Phi d\Omega, \tag{3.2}$$

where Φ is a testing basis function. Note that the operator $\mathcal{L}$ is symmetric with respect to its arguments. [Assuming that the outer boundary of the computational domain Ω is far away, we apply the magnetic isolation boundary condition $A_z = 0$ at $\partial\Omega$.] Knowing the solution A_z from Eq. (3.2), we solve an adjoint equation

$$\mathcal{L}(A_z^a, \Phi) = w_m \frac{1}{\mu_0} \int_{\Omega_m} \nabla A_z^* \cdot \nabla \Phi d\Omega + w_c \omega\sigma \int_{\Omega_c} A_z^* \cdot \Phi d\Omega. \tag{3.3}$$

The adjoint equation has exactly the same bilinear operator $\mathcal{L}$ as the direct equation, but with different source terms. It can be shown, in a similar way as in Ref. [8], that the first variation of our objective function, with respect to the shape displacement $d\xi$, is computed as a surface integral from solutions to the direct and the adjoint equations (3.2)-(3.3)

$$\delta\mathcal{E} = \int_\Gamma \left\{ \Re\left[\frac{1}{\mu_0}\nabla A_z \cdot \nabla A_z^a - \frac{1}{\mu_c}\nabla A_z \cdot \nabla A_z^a - j\omega\sigma A_z A_z^a \right] + w_c \frac{\omega\sigma}{2}|A_z|^2 \right\} d\xi d\Gamma. \tag{3.4}$$

Note that due to the field discontinuity (when $\mu_c \neq \mu_0$), the first two terms in the integrand in (3.4) should be evaluated separately from the air and the conductor side of the boundary Γ. This continuous formulation works for both conducting and ferromagnetic shielding materials. However, in our numerical example, we consider only a conducting shield with $\mu_c = \mu_0$.

For a given parameterization such as (2.3)-(2.4), the gradient with respect to the design parameters $\vec{c}$ is computed using the chain rule

$$\frac{\partial\mathcal{E}}{\partial c_k} = \sum_i \frac{\partial\mathcal{E}}{\partial\xi_i}\frac{\partial\xi_i}{\partial c_k}, \tag{3.5}$$

where the summation is performed for all (discretized) segments along the conductor boundary Γ.

In 3D, the continuum sensitivity is derived in a similar way. The final expression reads

$$\delta\mathcal{E} = \int_\Gamma \left\{ \Re\left[\frac{1}{\mu_0}\nabla\times\vec{A}^*\cdot\nabla\times\vec{A}^a - \frac{1}{\mu_c}\nabla\times\vec{A}^*\cdot\nabla\times\vec{A}^a - j\omega\sigma\vec{A}\cdot\vec{A}^a \right] + w_c\frac{\omega\sigma}{2}|\vec{A}|^2 \right\} d\xi d\Gamma,$$

where $\vec{A}$ and $\vec{A}^a$ are solutions to the direct and the adjoint 3D eddy current problems, respectively. These 3D problems can be efficiently solved using an ungauged AV formulations with edge elements [10].

We emphasize that the continuum gradient (3.5) is computed by solving the direct and the adjoint problems (3.2)-(3.3) *once* at each iteration, whereas to obtain the gradient by finite differencing, we need to solve the direct problem (3.2) as many times as the total number of design parameters. Furthermore, continuum sensitivity does not introduce numerical errors due to finite differencing. These errors may make the searching direction not optimal, especially when the solution is close to the (local) extreme point.

4. Numerical results

Equations (3.2) and (3.3) are solved using the commercial software FEMLAB [9], with quadratic Lagrange finite elements. For optimization, we use the Matlab routine 'fmincon' which pursues constrained optimization based on the sequential quadratic programming (SQP) method.

Figure 2 shows the total energy, defined by Eq. (2.2), versus the number of function evaluations, in the optimization process for the reference case with a symmetric shape. The total energy

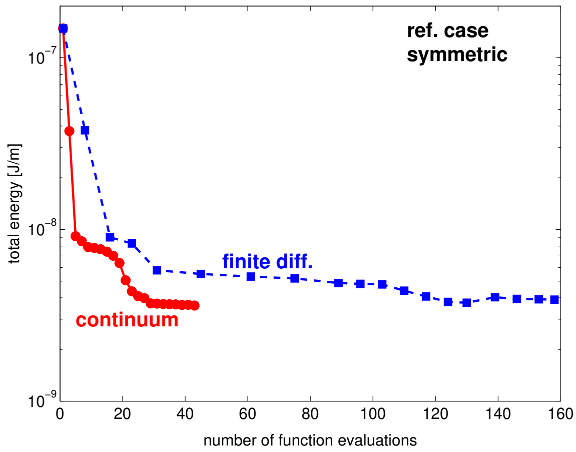

FIGURE 2. Compare the optimization process with continuum gradients (solid line) and with gradients by finite differencing (dashed line). The total energy is plotted against the accumulated number of function evaluations at each iteration.

is reduced by more than 40 times with the optimal shape. For comparison, we also plot results with the gradient computed by finite differencing. The continuum sensitivity shows clear advantage in terms of computational efficiency. This becomes even more pronounced as the number of design parameters increases.

The optimal shape for the above case is shown in Fig. 3(a). Shown also is the amplitude of the eddy current density induced in the shield. The optimal shape (and position) of the conductor is significantly different from the initial one. In fact, the optimal solution tries to push the shield close to the region of interest, instead of shielding the sources. The linear constraint on the highest position along the y-axis, as well as the nonlinear constraint on the total area of the conductor, is reached. For a comparison, Fig. 3(b) shows the optimal shape using the asymmetric parameterization.

Figure 4 shows the amplitude of the magnetic field along the bottom line of the region of interest. Four cases are compared – without the shield, with the initial rectangular shield, with optimal symmetric shield, and with optimal asymmetric shield. For the two reference cases, optimal shielding reduces the field by about 20 times compared with the no-shield field, and by about 5-6 times compared with the field using the initial rectangular shield. The asymmetric shape yields (in average) slightly better shielding than the symmetric one. On the other hand, the latter does not depend on the phase configuration (RST vs. RTS) of the source current.

By varying the number N of basis functions representing the conductor shape (keeping a uniform thickness), we find that for the symmetric (asymmetric) case, the first 4 (7) Legendre polynomials give good enough results. Further increasing N does not improve the results.

We also find that the minimum total energy is not sensitive to the parameter M from Eq. (2.4), as shown by Fig. 5. However, the optimal shape becomes more complicated with increasing M.

In Fig. 6 and 7, we vary the total area of conductor $A_{\max}$, while keeping four symmetric basis functions for the shape and $M = 0$. The optimal shape and the achieved field reduction are

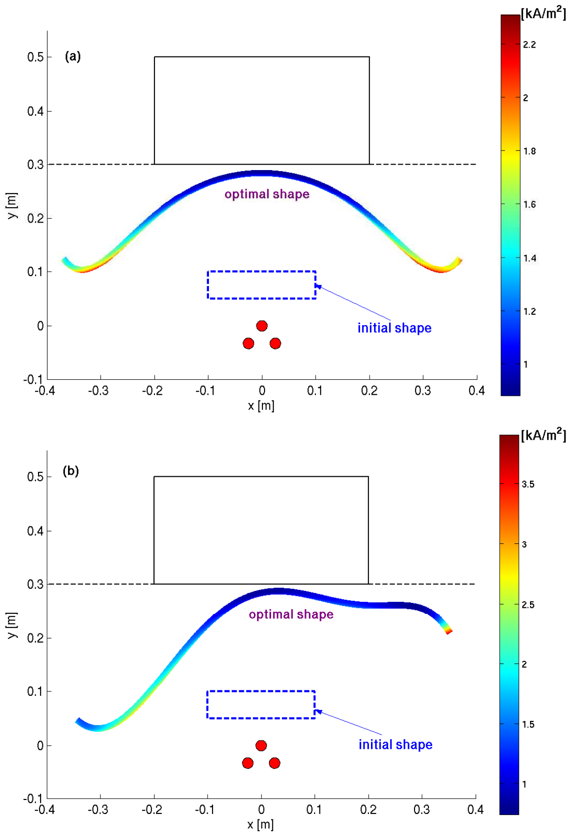

FIGURE 3. The optimal shape of the conducting plate for two reference cases, with symmetric (top) and asymmetric (bottom) parameterization, respectively.

very sensitive to the total area. Decreasing the amount of the shielding material results in more complicated optimal shape with thinner plate. It is interesting to observe that the minimum total energy is well approximated by $\mathcal{E} \propto A_{\text{max}}^{-1.8}$.

5. CONCLUSION

We have developed a continuum sensitivity based formulation for the shape optimization of shielding plates, in order to minimize the magnetic field at power frequencies. This formulation has been tested on a 2D example of reducing the magnetic field from a system of three-phase underground cables. The continuum gradient based optimization is very efficient. For the reference cases considered here, the optimally shaped conductor reduces the field amplitude by a factor of 20, compared with the no-field field. The optimal asymmetric shape works only slightly better than the symmetric one. The optimization yields good results with few number of Legendre basis functions. Increasing the amount of shielding material results in a significant field reduction.

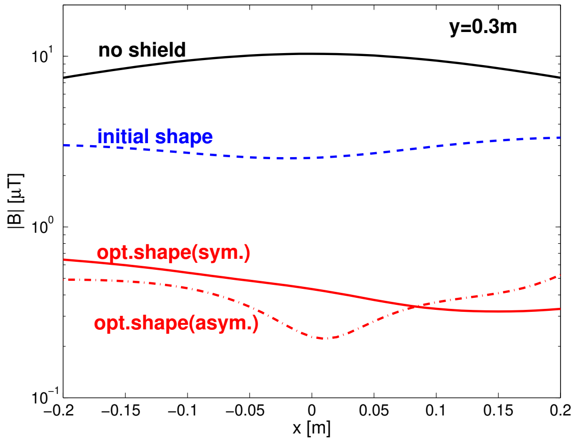

FIGURE 4. Amplitude of the magnetic field plotted along the bottom line of the region of interest ($y = 0.3$m), for four cases: without the shield, with initial rectangular-shaped shield, with optimal symmetrically shaped shield, and with optimal asymmetrically shaped shield.

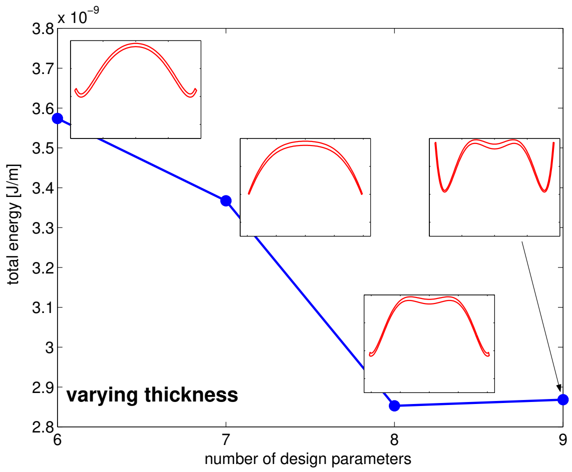

FIGURE 5. The minimum energy achieved by allowing a non-uniform thickness of the shielding plate. The number of design parameters for the bottom boundary of the conductor is 4. The number of parameters for the thickness M increases from 0 to 3.

REFERENCES

[1] H. Igarashi, A. Kost, T. Honma, "A three dimensional analysis of magnetic shielding with thin layers," Proceedings of 7th Int. IGTE Symposium, Graz, Austria, 1996.

[2] E. Salinas, "Conductive and Ferromagnetic Screening of 50 Hz Magnetic Fields from a Three-Phase System of Busbars," Journal of Magnetism and Magnetic Materials, vol. 226-230, pp. 1239-1241, 2001.

[3] A. Canova, G. Gruosso, M. Repetto, "Magnetic design optimization and objective function approximation," *IEEE Trans. Magn.*, vol. 39(5), pp. 2154-2162, Sept. 2003.

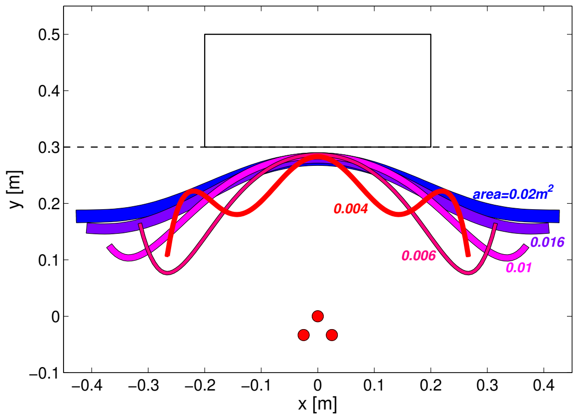

FIGURE 6. The optimal shape of the shielding plate with various values of the constraint on the total area. Symmetric parameterization is considered.

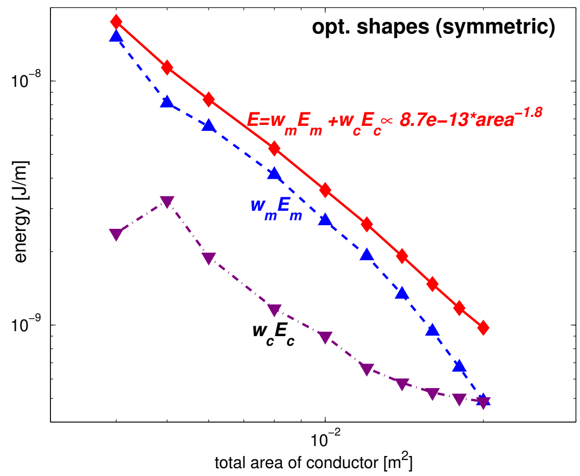

FIGURE 7. The minimum energy achieved with various values of the constraint on the total area of the shielding plate. Symmetric parameterization is considered.

[4] Y.Y. Yao, J.S. Ryu, C.S. Koh, and D.X. Xie, "Robust 3-D shape optimization of electromagnetic devices by combining sensitivity analysis and adaptive geometric parameterization," *IEEE Trans. Magn.*, vol. 40(2), pp. 1200-1203, March 2004.

[5] I.H. Park, B.T. Lee, and S.Y. Haln, "Sensitivity analysis based on analytic approach for shape optimization of electromagnetic devices: interface problem of iron and air," *IEEE Trans. Magn.*, vol. 27(5), pp. 4142-4145, Sept. 1991.

[6] S.Y. wang, S.K. Jeong, H.S. Yoon, "Continuum shape design sensitivity analysis of magnetostatic field using finite element method," *IEEE Trans. Magn.*, vol. 35(3), pp.1159-1162, May 1999.

[7] D.H. Kim, K.S. Ship, J.K. Sykulski, "Applying continuum design sensitivity analysis combined with standard EM software to shape optimization in magnetostatic problems," *IEEE Trans. Magn.*, vol. 40(2), pp. 1156-1159, March 2004.

[8] A. Bondeson, Y. Yang, and P. Weinerfelt, "Optimization of radar cross sections by a gradient method," *IEEE Trans. Magn.*, vol. 40(2), pp. 1260-1263, March 2004.
[9] http://www.comsol.com
[10] Yueqiang Liu, et al., "Eddy current computations using adaptive grids and edge elements," *IEEE transactions on Magnetics*, vol.38(2), pp. 449-452, March 2002.

CHALMERS FINITE ELEMENT CENTER PREPRINTS

2003–01	*A hybrid method for elastic waves* Larisa Beilina
2003–02	*Application of the local nonobtuse tetrahedral refinement techniques near Fichera-like corners* L. Beilina, S. Korotov and M. Křížek
2003–03	*Nitsche's method for coupling non-matching meshes in fluid-structure vibration problems* Peter Hansbo and Joakim Hermansson
2003–04	*Crouzeix–Raviart and Raviart–Thomas elements for acoustic fluid–structure interaction* Joakim Hermansson
2003–05	*Smoothing properties and approximation of time derivatives in multistep backward difference methods for linear parabolic equations* Yubin Yan
2003–06	*Postprocessing the finite element method for semilinear parabolic problems* Yubin Yan
2003–07	*The finite element method for a linear stochastic parabolic partial differential equation driven by additive noise* Yubin Yan
2003–08	*A finite element method for a nonlinear stochastic parabolic equation* Yubin Yan
2003–09	*A finite element method for the simulation of strong and weak discontinuities in elasticity* Anita Hansbo and Peter Hansbo
2003–10	*Generalized Green's functions and the effective domain of influence* Donald Estep, Michael Holst, and Mats G. Larson
2003–11	*Adaptive finite element/difference method for inverse elastic scattering waves* Larisa Beilina
2003–12	*A Lagrange multiplier method for the finite element solution of elliptic domain decomposition problems using non-matching meshes* Peter Hansbo, Carlo Lovadina, Ilaria Perugia, and Giancarlo Sangalli
2003–13	*A reduced P^1–discontinuous Galerkin method* R. Becker, E. Burman, P. Hansbo, and M.G. Larson
2003–14	*Nitsche's method combined with space–time finite elements for ALE fluid–structure interaction problems* Peter Hansbo, Joakim Hermansson, and Thomas Svedberg
2003–15	*Stabilized Crouzeix–Raviart element for the Darcy-Stokes problem* Erik Burman and Peter Hansbo
2003–16	*Edge stabilization for the generalized Stokes problem: a continuous interior penalty method* Erik Burman and Peter Hansbo
2003–17	*A conservative flux for the continuous Galerkin method based on discontinuous enrichment* Mats G. Larson and A. Jonas Niklasson

2003–18 *CAD–to–CAE integration through automated model simplification and adaptive modelling*
K.Y. Lee, M.A. Price, C.G. Armstrong, M.G. Larson, and K. Samuelsson

2003–19 *Multi-adaptive time integration*
Anders Logg

2003–20 *Adaptive computational methods for parabolic problems*
Kenneth Eriksson, Claes Johnson, and Anders Logg

2003–21 *The FEniCS project*
T. Dupont, J. Hoffman, C. Johnson, R.C. Kirby, M.G. Larson, A. Logg, and R. Scott

2003–22 *Adaptive finite element methods for LES: Computation of the mean drag coefficient in a turbulent flow around a surface mounted cube using adaptive mesh refinement*
Johan Hoffman

2003–23 *Adaptive DNS/LES: a new agenda in CFD*
Johan Hoffman and Claes Johnson

2003–24 *Multiscale convergence and reiterated homogenization of parabolic problem*
Anders Holmbom, Nils Svanstedt, and Niklas Wellander

2003–25 *On the relationship between some weak compactnesses with different numbers of scales*
Anders Holmbom, Jeanette Silfver, Nils Svanstedt, and Niklas Wellander

2003–26 *A posteriori error estimation in computational inverse scattering*
Larisa Beilina and Claes Johnson

2004–01 *Computability and adaptivity in CFD*
Johan Hoffman och Claes Johnson

2004–02 *Interpolation estimates for piecewise smooth functions in one dimension*
Anders Logg

2004–03 *Estimates of derivatives and jumps across element boundaries for multi-adaptive Galerkin solutions of ODEs*
Anders Logg

2004–04 *Multi-adaptive Galerkin methods for ODEs III: Existence and stability*
Anders Logg

2004–05 *Multi-adaptive Galerkin methods for ODEs IV: A priori error estimates*
Anders Logg

2004–06 *A stabilized non-conforming finite element method for incompressible flow*
Erik Burman and Peter Hansbo

2004–07 *On the uniqueness of weak solutions of Navier-Stokes equations: Remarks on a Clay Institute prize problem*
Johan Hoffman and Claes Johnson

2004–08 *A new approach to computational turbulence modeling*
Johan Hoffman and Claes Johnson

2004–09 *A posteriori error analysis of the boundary penalty method*
Kenneth Eriksson, Mats G. Larson, and Axel Mlqvist

2004–10 *A posteriori error analysis of stabilized finite element approximations of the helmholtz equation on unstructured grids*
Mats G. Larson and Axel Mlqvist

2004–11 *Adaptive variational multiscale methods based on a posteriori error estimation*
Mats G. Larson and Axel Mlqvist

2004–12 *Multi-adaptive Galerkin methods for ODEs V: Stiff problems*
Johan Jansson and Anders Logg

2004–13 *Algorithms for multi-adaptive time-stepping*
Johan Jansson and Anders Logg

2004–14 *Simulation of mechanical systems with individual time steps*
Johan Jansson and Anders Logg

2004–15 *Computational modeling of dynamical systems*
Johan Jansson, Claes Johnson, and Anders Logg

2004–16 *Adaptive variational multiscale methods based on a posteriori error estimation: Duality techniques for elliptic problems*
Mats G. Larson and Axel Mlqvist

2004–17 *Ultraconvergence of an interpolated finite element method for some fourth-order elliptic problems*
Andrey B. Andreev and Milena R. Racheva

2004–18 *Adaptive variational multiscale methods based on a posteriori error estimation: energy norm estimates for elliptic problems*
Mats G. Larson and Axel Mlqvist

2004–19 *Stabilized Lagrange multiplier methods for elastic contact with friction*
Per Heintz and Peter Hansbo

2005–01 *A posteriori error estimates for mixed finite element approximations of elliptic problems*
Mats G. Larson and Axel Mlqvist

2005–02 *On the numerical modeling of quasi-static crack growth in linear elastic fracture mechanics*
Per Heintz

2005–03 *Irreversibility in reversible systems I: the compressible Euler equations in 1d*
Johan Hoffman and Claes Johnson

2005–04 *Irreversibility in reversible systems II: the incompressible Euler equations*
Johan Hoffman and Claes Johnson

2005–05 *A Compiler for Variational Forms*
Robert C. Kirby and Anders Logg

2005–06 *Topological optimization of the evaluation of finite element matrices*
Robert C. Kirby, Anders Logg, L. Ridgway Scott and Andy R. Terrel

2005–07 *Modeling of resistive wall mode and its control in experiments and ITER*
Yueqiang Liu, M.S. Chu, A.M. Garofalo, Y. Gribov, M. Gryaznevich, T.C. Hender, D.F. Howell, R.J. La Haye, M. Okabayashi, S.D. Pinches, H. Reimerdes, P. de Vries, and EFDA-JET contributors

2005–08 *Continuum gradient based shape optimization of conducting shields for power frequency magnetic field mitigation*
Yueqiang Liu, P. Sousa Jr., E. Salinas, P. Cruz and J. Daalder

These preprints can be obtained from

`www.phi.chalmers.se/preprints`